

Joseph A. Frank, MD
John L. Ostuni, PhD
Yihong Yang, PhD
Yoseph Shiferaw, PhD
Anand Patel, BS
Jiangning Qin, PhD
Venkata S. Mattay, MD
Bobbi K. Lewis, BA
Ronald L. Levin, PhD
Jeff H. Duyn, PhD

Index terms:

Brain, blood flow, 10.121416,
10.121419
Brain, MR, 10.121416, 10.121419
Brain neoplasms, MR, 10.121416,
10.121419
Magnetic resonance (MR),
technology, 10.12144

Radiology 1999; 210:260–268

¹ From the Laboratory of Diagnostic Radiology Research, Clinical Center (J.A.F., J.L.O., Y.Y., B.K.L., A.P., J.Q., R.L.L., J.H.D.), the in Vivo NMR Research Center, National Institute of Neurological Disorders and Stroke (Y.S.), and the Clinical Brain Disorders Branch, National Institute for Mental Health (J.A.F., V.S.M.), National Institutes of Health, Bldg 10, Rm B1N256, 10 Center Dr, MSC 1074, Bethesda, MD 20892-1074. Received March 19, 1998; revision requested May 12; revision received May 28; accepted August 17. Address reprint requests to J.A.F.

© RSNA, 1999

Author contributions:

Guarantor of integrity of entire study, J.A.F.; study concepts, J.A.F.; study design, J.A.F., J.L.O., J.H.D., R.L.L.; definition of intellectual content, J.A.F., J.H.D., J.L.O.; literature research, J.A.F.; clinical studies, Y.Y., J.L.O., B.K.L., Y.S., V.S.M.; experimental studies, J.A.F., Y.Y., J.L.O., J.Q., J.H.D., R.L.L., Y.S., A.P.; data acquisition, Y.S., Y.Y., B.K.L., J.L.O.; data analysis, J.L.O., B.K.L.; statistical analysis, J.L.O., J.Q.; manuscript preparation, J.A.F.; manuscript editing and review, J.A.F., J.L.O., J.H.D.

Technical Solution for an Interactive Functional MR Imaging Examination: Application to a Physiologic Interview and the Study of Cerebral Physiology¹

Studies with functional magnetic resonance (MR) imaging produce large unprocessed raw data sets in minutes. The analysis usually requires transferring of the data to an off-line workstation, and this process frequently occurs after the subject has left the MR unit. The authors describe a hardware configuration and processing software that captures whole-brain raw data files as they are being produced from the MR unit. It then performs the reconstruction, registration, and statistical analysis, and displays the results in seconds after completion of the MR image acquisition.

Functional magnetic resonance (MR) imaging facilitates the study of dynamic physiologic processes by measuring the changes in MR signal intensity during rapidly acquired serial imaging. Functional MR imaging studies can be used to determine the following: (a) relative cerebral blood volume and relative cerebral blood flow by means of dynamic contrast material-enhanced MR imaging (1–11); (b) absolute cerebral blood flow by means of spin-tagging techniques (12–16); and (c) localized increases of neuronal activity in response to neurophysiologic stimulation by means of blood-oxygenation-level-dependent contrast (17–25). By using rapid imaging techniques, such as single-shot echo-planar or spiral imaging, each functional MR imaging study usually acquires large raw data sets, which

comprise hundreds or thousands of images, in relatively short periods of time (18,24,25). These data sets are usually not reconstructed on the MR imaging unit, since in most cases reconstruction would interfere with or delay the start of subsequent functional MR imaging experiments. Instead, the raw data are stored and subsequently transferred to an off-line workstation for analysis, which usually occurs long after the subject has left the MR unit (21–25). Given the cost of MR imaging examination time, it is unsatisfactory for both the researcher and/or the subject to complete an examination only to find that the functional MR imaging results are inadequate due to motion artifacts or poor compliance as a result of inadequate understanding of the paradigm. Thus, it is essential to develop a hardware system along with postprocessing techniques to display statistical results of the functional MR imaging study coregistered on anatomic images and thereby allow the rapid evaluation and preliminary interpretation of the experimental results.

Conceptually, a functional MR imaging-based physiologic interview consists of a group of experiments performed during a single imaging session in which the researcher can evaluate the data from any or all experiments at an early stage while the subject is in the MR imaging unit. This approach would enable the researcher to manipulate the activation paradigm for subsequent experiments. For example, results of a whole-brain blood-oxygenation-level-dependent activation experiment with isotropic voxels (17,18,24) could guide the planning of a subsequent perfusion experiment (ie, dynamic contrast enhancement or spin tagging). These

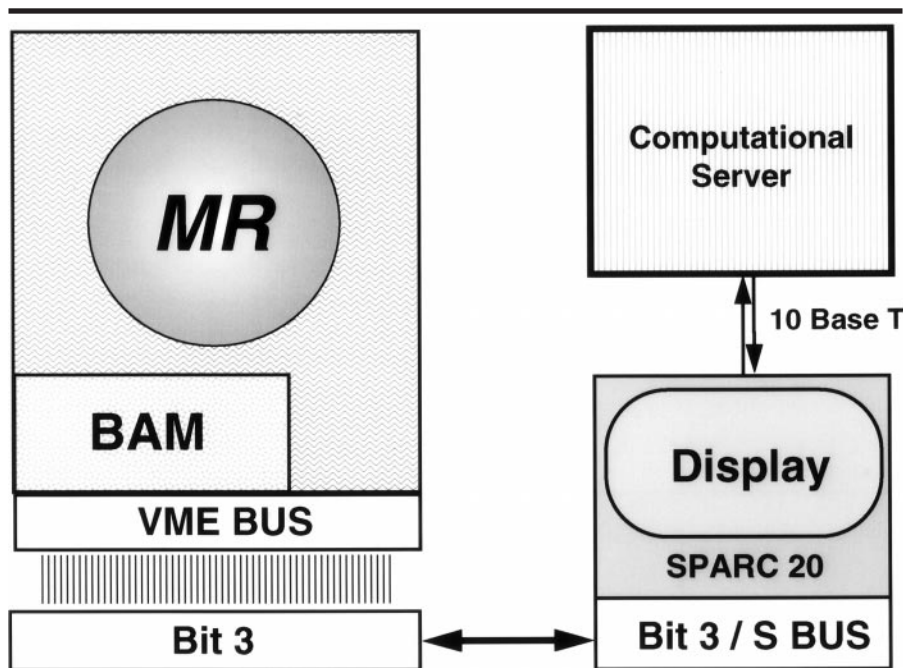


Figure 1. Schematic diagram of the hardware interface between the MR unit and the computational server and display system. *BAM* = bulk access memory.

types of studies, all performed in a single examination session, would allow the investigator to review the blood-oxygenation-level-dependent activation map and then to either vary the work load of the task or repeat the study multiple times to observe changes associated with reproducibility, learning, or precision.

The purpose of this study was to evaluate a hardware and software configuration that costs less than most MR hardware upgrades and rapidly performs the following tasks: (a) captures the raw image data on the fly, (b) reconstructs the image files, (c) registers all volumes, and (d) performs a predefined statistical analysis for either a blood-oxygenation-level-dependent functional MR imaging study or a dynamic contrast-enhanced study. Relevant maps are displayed in seconds after the completion of the MR acquisition.

Materials and Methods

Hardware Requirements

Functional MR imaging studies were performed on a clinical 1.5-T MR unit (Echo Speed; GE Medical Systems, Milwaukee, Wis) equipped with fast gradient hardware. The computer hardware configuration was based on a recently reported real-time cardiac MR imaging system (26). On the MR host computer, the disk space for the raw data was increased

to 2 Gbyte with a third-party magnetic drive. A Bit3 VME bus adapter card (Bit3 Computer, Minneapolis, Minn) was added to the MR unit to enable access to the image raw data stored in the bulk access memory, or BAM. A schematic representation of the hardware configuration is shown in Figure 1. An SBus Bit3 board was also installed into another Unix workstation computer (SPARC 20; Axil Computer, Concord, Mass) and connected to the bus adapter card on the MR unit. This connection facilitated the rapid transfer, via the Unix workstation, of raw data sets from the MR unit to the computational server, which had four processors (DEC Alpha 4100 equipped with 21164/400 chips; Digital Equipment, Maynard, Mass). The Sparc 20 Unix workstation played two major roles: (a) to synchronize the data input and output, the workstation serving as a data buffer between the MR unit and the computational server, and (b) it performed byte swapping of the data from the imager. This latter role was necessary due to the incompatibility in the representation of the data between the imager and the computational server. The computational server was equipped with four 433-MHz computer processing units, 1 Gbyte of shared RAM, and 16-Gbyte magnetic disk drive. The hardware configuration is not a unique solution because it has been designed to interface with the specific MR unit hardware and output. Analogous computer hardware

configurations should be adaptable to most clinical imagers that are being used for functional MR imaging studies today, given an appropriate level of cooperation by the MR manufacturer.

Processing Software

After transferring the raw data to the RAM of the computational server, the following sequential computational steps were performed. (a) The images were reconstructed by interpolating the single-shot spiral data sets onto an orthogonal, equidistant grid (27), followed by a two-dimensional fast Fourier transformation. The interpolation consisted of a regridding algorithm with a Gaussian convolution window. (b) Images were registered with a high-speed optimized version of the registration algorithm known as correspondence of closest gradient voxels (28). The correspondence of the closest gradient voxels software package is a three-dimensional volume registration algorithm that aligns areas of high-intensity change on the basis of a rigid body transformation of the data sets. Of note, this particular regridding procedure allows reconstruction of data collected with arbitrary k-space trajectories, including the trajectories characteristic of spiral and echo-planar imaging (24).

For blood-oxygenation-level-dependent functional MR imaging studies, a normalization of the signal intensities across the volumes was performed. All volumes were normalized so that the mean intensity value of their relevant voxels were identical, which allowed comparison between studies. A baseline correction was applied on a voxel-by-voxel basis for all voxels in the brain with a third-order polynomial fit over the time series data (17). Calculation of the "activation" statistical map was done with an arbitrary user-defined threshold for the Student *t* test. For this study, all time points for a box-car paradigm were used in the statistical analysis to calculate the "activation" map, although any type of input function can easily be accommodated by the software, thereby allowing the researcher to delete data points to deal with the hemodynamic delay effect of changes in signal intensity observed with blood-oxygenation-level-dependent functional MR imaging. Voxels that were determined to be statistically significant different were superimposed in red onto the initial reconstructed functional MR imaging spiral volume and displayed automatically for investigator review. An s map, which is defined as the SEM of the

difference between the signal intensity on a voxel-by-voxel basis for all volumes in each epoch (ie, "on" and "rest" conditions) in a box-car paradigm, was also displayed for review. A histogram of the normalized SEM (ie, SEM of the difference between the two means ["on" vs "off"] condition at each voxel divided by the mean signal intensity over time) of all voxel signal intensity was also plotted in a second window and displayed automatically in the MR control room (17,18).

For the dynamic contrast-enhanced studies, maps of relative cerebral blood volume, relative cerebral blood flow, and time to peak intensity were calculated by fitting a gamma variate function to the signal intensity-time course (1,7-9,11,29,30). The fitting was performed for the voxels (50,000-150,000) in the brain. The map of time to peak intensity was obtained with an algorithm that searches for the occurrence of the maximum change in signal intensity over time, on a voxel-by-voxel basis. The arterial input function was obtained by searching all voxels in the brain for the greatest signal intensity change and then selecting the voxels with the earliest change in time to peak signal intensity, as reported by Petrella et al (8). The average gamma variate fit for the voxels meeting these two criteria was then used for the arterial input function. The deconvolution was performed with a robust algorithm based on the singular value decomposition algorithm described by Ostergaard et al (29,30). The relative cerebral blood volume, relative cerebral blood flow, and time to peak intensity are all automatically displayed for the researchers review.

Cerebral blood flow images, acquired with either arterial spin tagging or multi-section flow-sensitive alternating inversion recovery, were processed in a similar manner to the blood-oxygenation-level-dependent functional MR imaging studies (12-16,31). For these studies, a T1 map was created during a separate acquisition, and these images were registered to the functional MR imaging study. As with the blood-oxygenation-level-dependent functional MR imaging studies, the percentage change in cerebral blood flow was determined by taking the difference between the activation and rest states in response to a neurophysiologic stimulus. Since the requirements to perform arterial spin tagging or flow-sensitive alternating inversion-recovery studies are similar to those for blood-oxygenation-level-dependent and dynamic contrast-enhanced studies, these experiments were not included in this study.

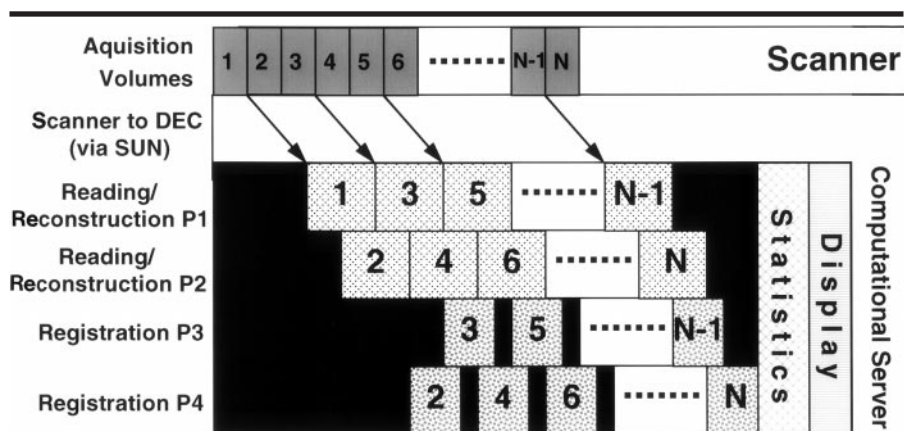


Figure 2. Schematic diagram of four-processor computational server with respect to interactive functional MR imaging system. P1-P4 represent processor numbers. For a blood-oxygenation-level-dependent study, the statistics and display steps take 20 seconds after the completion of the raw data acquisition. For a dynamic contrast-enhanced study, the statistics step takes about 29 seconds, during which the changes in signal intensity for each voxel in the brain are fitted with a gamma variate function to determine the relative cerebral blood volume. The maximum change in signal intensity over time is used to determine the map of time to peak intensity. A search is performed for the arterial input function, and the deconvolution is performed with the singular-value decomposition algorithm to determine the relative cerebral blood flow (29,30). It takes another 17 seconds to display the maps, for a total time of 49 seconds after the completion of the raw data acquisition. DEC = Digital Equipment Corp (computational server), SUN = Sparc 20 Unix workstation.

The image processing was optimized in a pipeline software design with a throughput that matched the speed of the raw data acquisition rate of the MR unit (Fig 2). Software algorithms for the parallel processor were written in C++ (Bjarne Stroustrup, Bell Laboratories, Murray Hill, NJ) with a TCL/TK interface (John Ousterhout, University of California, Berkeley). It should be noted that only single processor versions of the reconstruction and registration software were used, thus minimal software rewriting was necessary to take advantage of the multiprocessor architecture. The user interface allowed selection of the type of MR pulse sequence used (eg, echo-planar or spiral imaging), the type of study performed (eg, blood-oxygenation-level-dependent, dynamic contrast-enhanced, spin tagging), the number of whole-brain volumes acquired, the matrix size, the paradigm definition (ie, time and number of each on-off cycle, data to be included or excluded to compensate for hemodynamic factors), and the statistical thresholds. This interface also allowed the user to display certain data, such as motion correction, that are not automatically displayed at the end of each study. Moreover, the software was written to accept raw image files directly from the MR imaging unit, from storage on the hard disk, or from tape.

MR Imaging

To allow the highest image acquisition rate within the constraints of the imager

gradient hardware, a multisection single-shot spiral imaging acquisition technique was used for all functional MR imaging modalities. With the maximum gradient slew rate of 120 T/m/sec and the maximum gradient amplitude of 22 mT/m, the minimal acquisition window was 22 msec (18,24) for a 64 × 64 matrix and a 240-mm field of view, and the maximum acquisition rate was 30 sections per second. Under the same conditions, the duration of the acquisition window for echo-planar imaging was 35 msec. For both the blood-oxygenation-level-dependent and the dynamic contrast-enhanced functional MR imaging studies, multisection single-shot gradient-echo spiral images were obtained. The whole brain was covered in 2 seconds per volume with a nominal in-plane resolution of 3.75 × 3.75 mm, echo time of 35 msec, repetition time of 55.6 msec, 36 sections, section thickness of 4 mm, and flip angle of 84°. The total acquisition time for a blood-oxygenation-level-dependent functional MR imaging study was 4.13 minutes and for a dynamic contrast-enhanced functional MR imaging study was 2.67 minutes. Finger-tapping activation paradigms described previously (17) were used to evaluate the system performance. For dynamic contrast-enhanced studies, gadopentetate dimeglumine (Magnevist; Berlex Laboratories, Wayne, NJ) at 0.1 to 0.2 mmol per kilogram of body weight was injected at 10 mL/sec with a MR imaging-compatible mechanical injector

(Spectris; Medrad, Pittsburgh, Pa). Imaging was started approximately 15–20 seconds before injection to obtain baseline images.

All clinical studies were performed under an approved intramural review board protocol at the National Institutes of Health. Informed consent was obtained for all functional MR imaging studies.

For this study, 10 healthy control subjects (eight men and two women; age range, 22–56 years; mean age, 35.8 years) and five patients with central nervous system malignancies (three men and two women; age range, 24–68 years; mean age, 53.4 years) were evaluated with the functional MR imaging interactive techniques as part of brain activation studies or imaging work-up before neurosurgery.

■ Results

For a blood-oxygenation-level-dependent functional MR imaging study, the following performance characteristics of the system configuration divide the various tasks over the four processors: 36-section volume acquisition time, 2.0 seconds per volume; raw data volume size, 792,000 B; processor read volumes (processors 1 and 2), 0.5 seconds per volume; reconstruction (processors 1 and 2), 1.5 seconds per volume; registration (processors 3 and 4), 1.5 seconds per volume; normalization of the signal intensities across the volumes, baseline correction, and statistics (processors 1–4), 10 seconds; display t maps with images, 7 seconds; total functional MR acquisition (A) (124 volumes), 4 minutes 8 seconds; total processing time (B), 4 minutes 28 seconds; processing time after MR data collection ends (B – A), 20 seconds (including delay time for the first volume to be acquired completely and transferred over the bus adapter card); total processing time with a single processor (C), 15 minutes 28 seconds; and time ratio (C/B), 3.51. It takes approximately 4 minutes 8 seconds to acquire all 124 raw data volumes. During that acquisition time, the system processes the raw image files with essentially no delay. All 124 volumes are reconstructed and registered and the statistical analysis is performed and displayed with a running time of 4 minutes 28 seconds. Figure 2 is a schematic timing diagram for an interactive functional MR imaging examination.

The data from blood-oxygenation-level-dependent functional MR imaging studies that were processed with this system produced reliable and reproducible

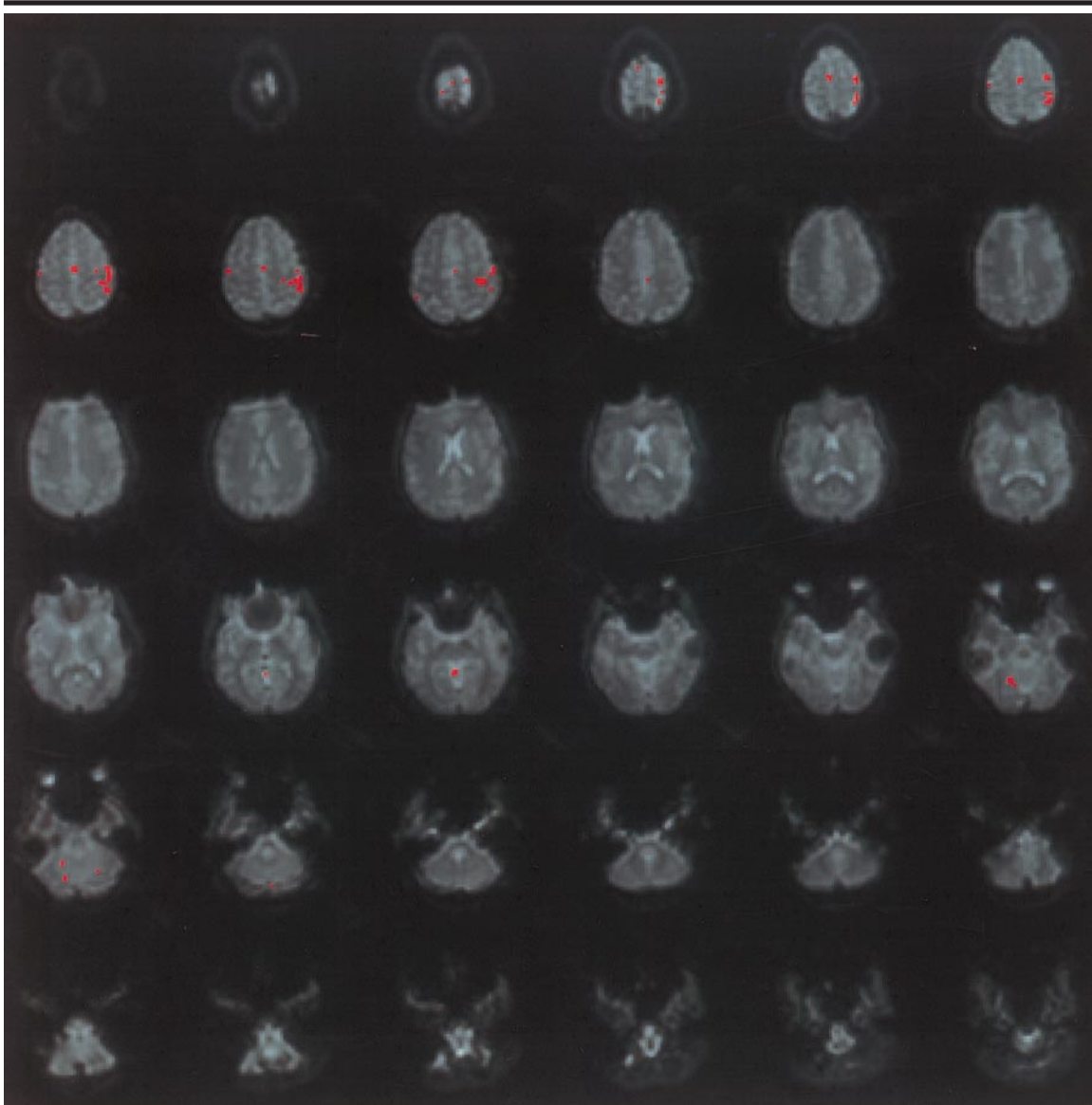
results. Furthermore, the results were consistent with activation maps obtained with conventional processing strategies, which take hours of processing time (21,25). However, the major difference in producing the former activation maps (Fig 3) was a dramatic reduction in the time required to reconstruct and register the images. This reduction results in the ability to produce and display the activation t map, s map, and normalized SEM histogram 20 seconds after the completion of the MR data acquisition (Fig 3b). The normalized SEM histogram and a graph of patient motion, which was obtained from the registration of the images, are used as the criteria for rejecting a run or determining the necessity to repeat a given experimental run. The total processing time reported previously must be compared with the several minutes of downtime usually experienced when performing functional MR imaging studies. This delay is due to waiting for the array processor to finish reconstructing the images or writing the unprocessed raw data files to disk and subsequent transfer of the acquired data files, which are larger than 100 Mbyte, to an off-line workstation.

The computation time to process the large raw data files for blood-oxygenation-level-dependent functional MR imaging (eg, 124 volumes of $64 \times 64 \times 36$ sections) is 15 minutes 38 seconds to produce t maps. This time included the time for disk retrieval with a single processor on the computational server and the processing time with the software. When all four processors on the unit were used, the total processing time was 4 minutes 29 seconds. The use of all four processors represents approximately a 3.5-fold increase in speed in the data analysis, indicating the effective use of available computer processing units achieved with the C++ parallel software.

For a dynamic contrast-enhanced functional MR imaging study, the following performance characteristics of the system configuration divide the various tasks over the four processors: 36-section volume acquisition time, 2.0 seconds per volume; raw data volume size, 792,000 B; processor read volumes (processors 1 and 2), 0.5 seconds per volume; reconstruction (processors 1 and 2), 1.5 seconds per volume; registration (processors 3 and 4), 1.5 seconds per volume; calculation of maps of relative cerebral blood volume, time to peak intensity, and relative cerebral blood flow (processors 1–4), 29 seconds; display of maps, 17 seconds; total functional MR acquisition (A) (80 volumes), 2 minutes 40 seconds; total processing time (B), 3

minutes 29 seconds; processing time after MR data collection ends (B – A), 49 seconds (including delay time for the first volume to be acquired completely and transferred over the bus adapter card); total processing time with a single processor (C), 10 minutes 8 seconds; and time ratio (C/B), 2.92. The initial steps in the process are exactly the same as those for the blood-oxygenation-level-dependent functional MR imaging study, although for the former, fewer whole-brain volumes (about 80) are usually acquired over the 2 minutes 40 seconds. After the completion of the MR data acquisition, it takes 49 seconds to perform a voxel-by-voxel gamma variate fit of the time series data, search for the bolus time to peak intensity, determine the arterial input function used to calculate the relative cerebral blood flow maps, and display all three maps. Moreover, the time savings for creation of maps of relative cerebral blood volume, time to peak intensity, and relative cerebral blood flow is similar to that with the blood-oxygenation-level-dependent analysis when the raw data from the dynamic contrast-enhanced studies are processed from the disk with a single processor (processing time, 10 minutes 48 seconds) rather than with all four processors (processing time, 3 minutes 29 seconds).

Figure 3 is an example of a blood-oxygenation-level-dependent functional MR imaging study obtained in a control subject performing sensorimotor activation by finger tapping at 2 Hz with the dominant right hand. The data were processed with the hardware configuration described previously. The blood-oxygenation-level-dependent functional MR imaging study was repeated three times during the session. In the second experiment, the subject was asked to move during the examination. Figure 3b is the normalized SEM histograms from the three sequential studies. It is clear that the histogram from the second study has a wider distribution and is interpreted as an inadequate study, which precludes any further analysis of the data set. Another blood-oxygenation-level-dependent functional MR imaging data set was subsequently collected and analyzed to demonstrate the utility of the interactive nature of this type of system configuration. The difficulty with subject motion is that even when a registration algorithm finds the correct motion transformation, the ensuing interpolation reduces the high-frequency components in the registered volumes, thus increasing the SD at each voxel position (32). Figure 3c is a plot of the rotation motion correction applied



a.

Figure 3. Blood-oxygenation-level-dependent functional MR imaging study. (a) Activated voxels in red are superimposed on top of axial spiral images for the five motor regions (primary sensorimotor, lateral premotor, parietal, supplementary motor, and ipsilateral cerebellum) associated with right-handed, finger-tapping paradigm with a threshold of 4.8. Images were obtained within 20 seconds after completion of acquisition of the raw data. (*Fig 3 continues.*)

by the registration algorithm for the correspondence of closest gradient for the first and second experiments. For this experiment, the control subject was asked to begin the session with his or her head tilted to one side and then slowly rotate it to the other side during the course of the experiment. All subject motion is represented as a single rotation magnitude and a single translation magnitude. The axes of rotation and translation are not displayed.

Figure 4 is an example of a dynamic contrast-enhanced study in a control sub-

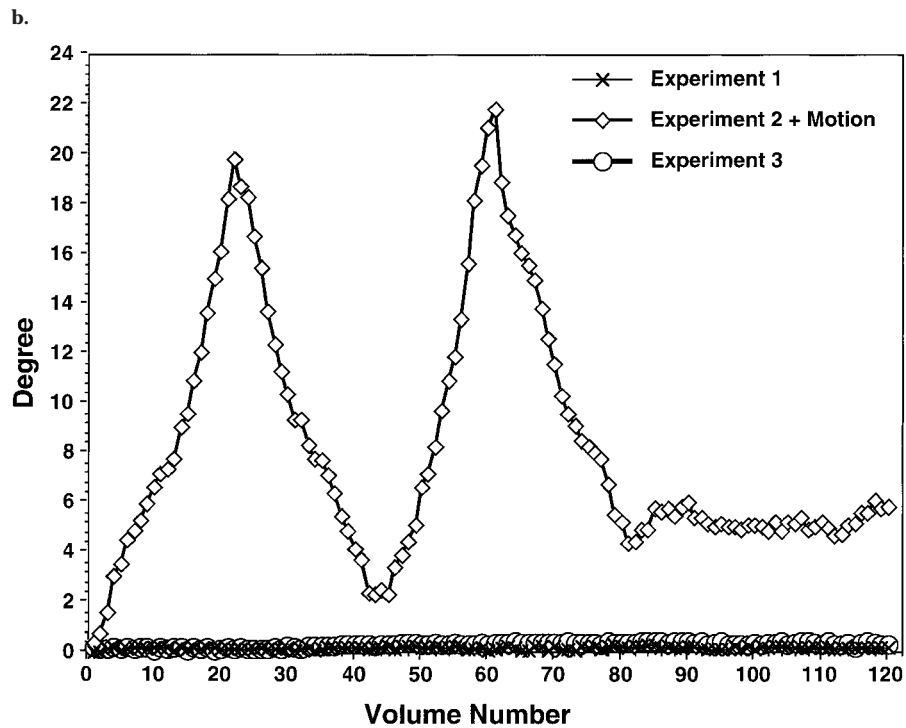
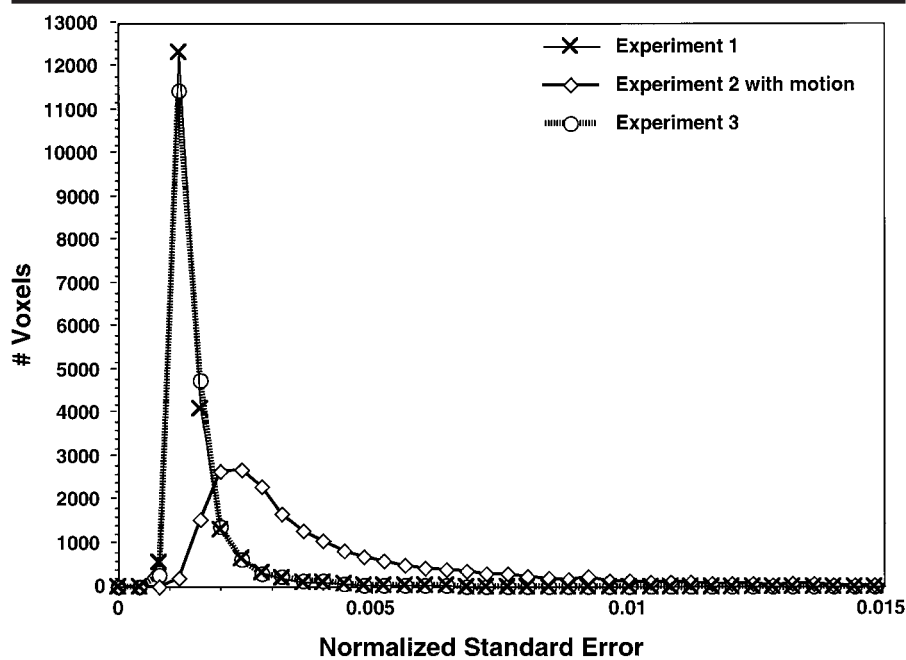
ject in which sample maps of relative cerebral blood volume, time to peak intensity, and relative cerebral blood flow are shown. In this study, approximately 99% of the voxels were successfully fitted with the gamma variate function. These maps are consistent with results obtained in a control subject.

Discussion

This article describes a hardware configuration and processing software that captures whole-brain raw data files as

they are being produced from the MR unit; performs reconstruction, registration, and statistical analysis; and displays results in seconds after completion of the MR image acquisition.

At our and other institutions, analysis of functional MR imaging data sets usually takes several hours to days (21,25) because of delays in the off-line reconstruction, registration, and subsequent statistical analysis of the raw image data. Time is also required to archive all unprocessed raw data image files and images. Although the most important part of this



c. **Figure 3 (continued).** (b) Plot of normalized SEM histograms for all voxel signal intensities over time. In experiment 2, the control subject was asked to move to simulate an uncooperative patient; results were plotted with the registration algorithm for the correspondence of closest gradient voxels applied to the data. Note the spread of the histograms for the second experiment as compared with that for the first and third experiments. (c) Graph displays the degree of rotation detected and corrected with the registration algorithm for the correspondence of closest gradient voxels for each experiment.

computation process lies in the ultimate analysis of the functional MR images, for which various software packages are available (33–36), the bulk of the initial time

commitment is spent in reconstruction, registration, and storage of the images. As a result of this process, even a quick review of activation maps usually occurs

long after the subject has left the imager. Owing to delays imposed by the MR unit, researchers tend to limit the number of experimental trials acquired during a 1-hour imaging session, in part because they are unsure of the reliability and integrity of their studies.

Dynamic contrast-enhanced MR imaging studies are usually performed once during an imaging session and are used as part of an early evaluation of an acute ischemic event or pathologic conditions of the central nervous system (1,6). These results may help monitoring of the treatment effects of antithrombolytic agents in acute stroke (4) and have been shown to help grading of primary malignancies of the central nervous system (16). Analysis of the maps of relative cerebral blood volume, time to peak intensity, and relative cerebral blood flow calculated in near real time after completion of the acquisition of the raw data may provide further insight into the efficacy of novel therapies.

Cox et al (21) recently reported the advantages of being able to view functional MR imaging data sets in near real time. The advantages included the abilities (a) to develop or modify activation paradigms quickly, allowing one to test hypotheses while the subject was still in the MR unit; (b) to examine the data for artifacts that may contaminate (ie, physiologic motion) the images; and (c) to develop new paradigms on-line, therefore making functional MR imaging a more flexible neurologic tool. Furthermore, to quickly display the analyzed results of blood-oxygenation-level-dependent, perfusion (ie, spin tagging), or dynamic contrast-enhanced functional MR imaging studies in near real time will also allow the evaluation of the subject's reaction to a provocative pharmacologic challenge (ie, Wada test). Real-time analysis would also permit a direct comparison with the subject's baseline condition (25). These data may provide valuable information about the neurologic integrity and functional status of the individual. It would also be possible to design sequential functional MR imaging examinations in which, for example, the results of an initial blood-oxygenation-level-dependent activation study would guide other functional (ie, spin tagging, dynamic contrast-enhanced) or metabolic imaging (37) examinations to a specific area of interest or to repeat the paradigm with changes such as higher spatial and/or temporal resolution (38).

With a real-time functional MR imaging approach, Cox et al (21) used an

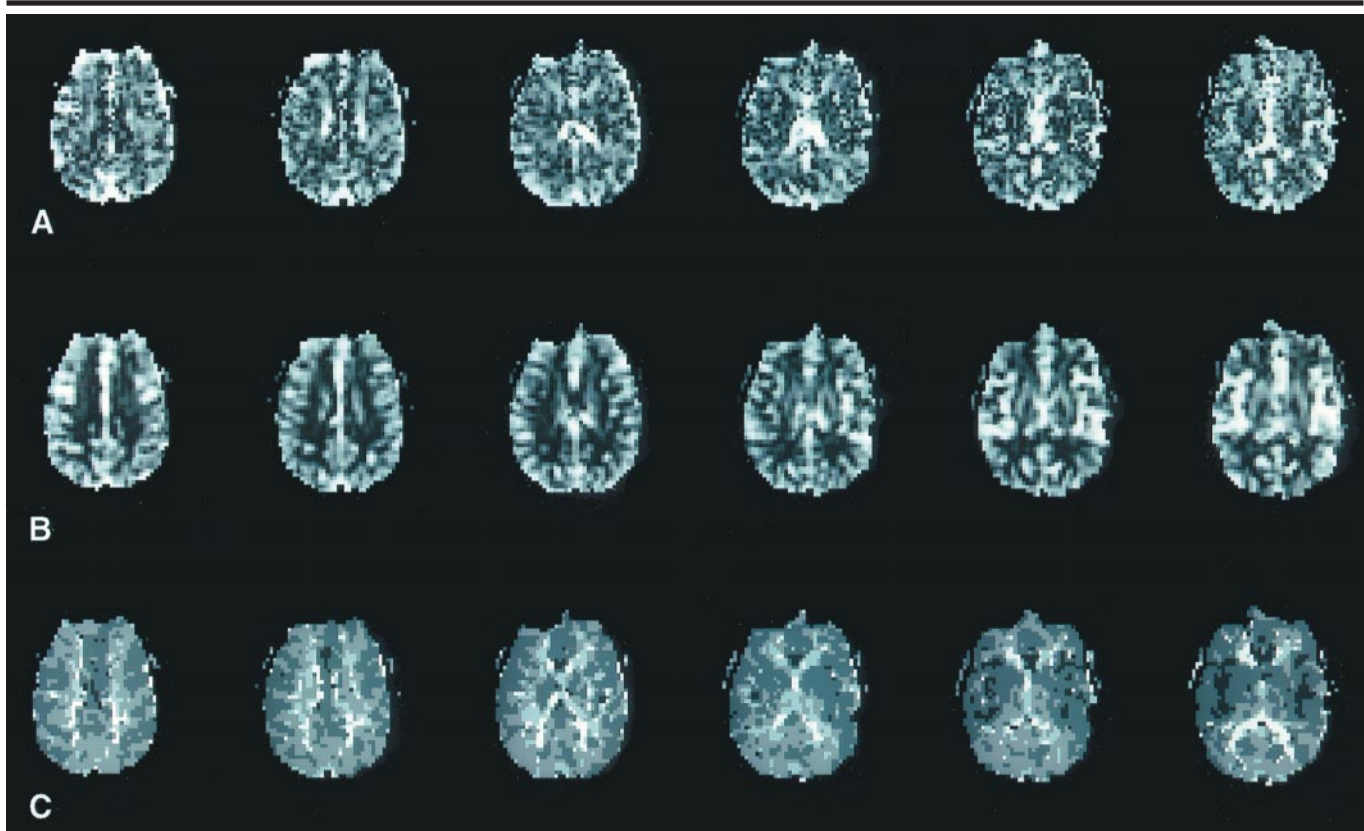


Figure 4. Dynamic contrast-enhanced study. Six representative maps from a 36-section whole-brain study performed in a 25-year-old male control subject after administration of 0.1 mmol of gadopentetate dimeglumine as a bolus at 10 mL/sec. A, Relative cerebral blood volume. B, Relative cerebral blood flow. C, Time to peak intensity. These maps were produced from 80 whole-brain spiral images and were displayed in 49 seconds after the completion of the study. Differences in gray and white matter in parts A and B can be clearly appreciated. The high signal intensity observed in part C indicates a delayed arrival (up to 5 seconds) of the bolus in the white matter, the choroid plexus, and the larger vessels such as sinuses compared to that in the arteries.

algorithm that recursively computes the correlation coefficient of an image sequence with a reference vector and simultaneously removes any undesired linear trend from the data. In their study, activation maps were displayed with a predetermined statistical threshold. This was performed at various time points during a blood-oxygenation-level-dependent, echo-planar study acquired at a single location while the subject performed a finger-tapping experiment. The authors indicated that their algorithm was not a complete substitute for postprocessing in which multiple statistical tests can be applied to the raw data sets to detect the activation and suppression of the artifacts (21). However, they indicated that the benefit of this approach is to look primarily for spuriously correlated artifacts. With the availability of near real-time imaging, one needs to avoid the temptation to truncate an experiment early because the statistical maps appear to give the results that the investigators required. Stopping rule criteria based on

the likelihood that the activation maps would be stable need to be developed before initiation of the functional MR imaging study to avoid the result of an arbitrary number of epochs collected, which would confound any type of intra- or intersubject comparisons. Clearly, such a decision should be avoided. Moreover, any stopping rule criteria developed for a real-time displayed functional MR imaging study would impose a more stringent (higher) threshold for statistical significance to define activation (39).

Real-time reconstruction and display of MR data has been used successfully to direct single-section, MR fluoroscopy-based imaging techniques to localize anatomic structures or guide and monitor interventional procedures (25,40–42). Kerr et al (26) recently demonstrated the utility of real-time interactive MR imaging with a conventional imager for abdominal and cardiac imaging. Use of this approach and a functional analysis will be required in the future to exploit the full potential of MR imaging as a means of

monitoring normal and abnormal physiologic responses to stress or specific tasks.

Although single-shot spiral imaging is not available on most clinical MR imagers, this pulse sequence requires more computation time to regrid and reconstruct the raw data into sections than is required for a standard rectilinear reconstruction, thereby potentially imposing a time delay in the data processing stream before starting image registration. However, with our system configuration, no appreciable delay was encountered (Fig 2). Furthermore, the single-shot, gradient-echo, spiral pulse sequence acquired images at a rate of greater than 18 sections per second. This rate placed an increased demand on the buffering and timing of the software pipeline to handle the raw data being transferred from the MR imaging unit to the hardware configuration used for rapidly processing and displaying of the acquired whole-brain functional MR imaging data sets.

The success of an interactive functional MR imaging-based physiologic interview

depends on the investigator being able (a) to review processed and statistically analyzed image maps shortly after completion of the MR acquisition and to determine (b) if the study needs to be repeated or (c) if a modification to the paradigm is required to further elucidate cerebral response. This sequence of events should occur while the subject is in the imager to take advantage of the experimental conditions. Our hardware configuration provided the neuroscientist with an initial analysis of large functional MR imaging data sets in seconds after completion of the MR acquisition.

This interactive system costs less than most major MR imaging hardware upgrades (ie, <\$100,000) but realistically provides researchers with a more efficient use of MR imager time, ultimately increasing the number of clinical and research studies performed. In the future, as less expensive multiprocessor desktop computers equipped with faster processing chips become available, it is likely that neuroscientists will be able to afford and therefore incorporate an interactive functional MR imaging examination into their clinical studies. Furthermore, the processing software should be able to be compiled on these less expensive multiprocessor desktop computers.

With additional hardware, we connected multiple MR imaging units to the computational server, thus allowing time sharing of the hardware configuration. Moreover, this system package facilitated the on-line planning and evaluation of various protocols (eg, spectroscopic imaging or dynamic contrast-enhanced maps of cerebral blood volume, arrival time or time to peak, and cerebral blood flow), and it could be used in conjunction with other modalities to study the effect of carotid stenosis on cerebral perfusion (11) or become part of a work-up for an acute brain attack protocol (1,5,43,44). It can also be used for adaptive task tuning (eg, increasing the stress load), repeating of unsuccessful images (eg, subject motion) used for brain mapping (12,18), presurgical planning of eloquent cortex relationship to a surgical target (3,23,25,40), and possibly other therapeutic interventions. It is important to note that the hardware can also function as a stand alone postprocessing unit and can be used with other compatible software packages for a more extensive statistical analysis of the functional MR imaging data set (33).

Ultimately, use of this type of interactive system is necessary for functional MR imaging techniques to be integrated into clinical practice, and it has the potential

to be used as a valuable tool to improve the care of patients with neurologic and psychiatric disorders.

Acknowledgments: The authors thank Tsur Bernstein, MD, Brad Burge, MD, and Carolyn Duffield, MD, from GE Medical Systems for their helpful support of this project. We also thank GE Medical Systems for the Bit3 board connection from the MR unit. We also thank John Pauly, MD, for the access computer software used in the data transfer from the MR unit.

References

1. Sorensen AG, Tievsky AL, Ostergaard L, Weisskoff RM, Rosen BR. Contrast agents in functional MR imaging. *JMRI* 1997; 7:47-55.
2. Bruening R, Kwong KK, Vevea MJ, et al. Echo-planar MR determination of relative cerebral blood volume in human brain tumors: T1 versus T2 weighting. *Am J Neuroradiol* 1996; 17:831-840.
3. Bruening R, Wu RH, Yousry TA, et al. Regional relative blood volume MR maps of meningiomas before and after partial embolization. *J Comput Assist Tomogr* 1998; 22:104-110.
4. Baird AE, Benfield A, Schlaug G, et al. Enlargement of human cerebral ischemic lesion volumes measured by diffusion weighted magnetic resonance imaging. *Ann Neurol* 1997; 41:581-589.
5. Tsuchida C, Yamada H, Maeda M, et al. Evaluation of peri-infarcted hypoperfusion with T1* weighted dynamic MRI. *JMRI* 1997; 7:518-522.
6. Aronen HJ, Glass J, Pardo FS, et al. Echo-planar MR cerebral blood volume mapping of gliomas: clinical utility. *Acta Radiol* 1995; 36:520-528.
7. Mattay VS, Weinberger DR, Barrios FA, et al. Brain mapping using functional MR imaging: comparison of gradient-echo-based exogenous and endogenous contrast techniques. *Radiology* 1995; 194:687-691.
8. Petrella JR, DeCarli C, Dagli M, et al. Assessment of whole brain vasodilatory capacity with acetazolamide challenge at 1.5 T using dynamic contrast imaging with FS-BURST. *Am J Neuroradiol* 1997; 18:1153-1161.
9. Petrella JR, DeCarli C, Dagli M, et al. Age related vasodilatory response to acetazolamide challenge in healthy adult humans: a dynamic contrast-enhanced MR perfusion imaging study. *Am J Neuroradiol* 1998; 19:39-44.
10. Duyn JH, Yang Y, Frank JA, Mattay VS, Hou L. Functional magnetic resonance neuroimaging: data acquisition techniques. *Neuroimage* 1996; 4(suppl):S76-S83.
11. Duyn JH, van Gelderen P, Barker P, Frank JA, Mattay VS, Moonen CTW. 3D bolus tracking with frequency-shifted BURST MRI. *J Comput Assist Tomogr* 1994; 18:680-687.
12. Williams DS, Detre JA, Leigh JS, Koretsky AP. Magnetic resonance imaging of perfusion using spin inversion of arterial water. *Proc Natl Acad Sci USA* 1992; 89:212-216.
13. Ye FQ, Smith AM, Yang Y, et al. Quantitation of regional cerebral blood flow increases during motor activation: a steady-

- state arterial spin tagging study. *Neuroimage* 1997; 6:104-112.
14. Ye FQ, Pekar JJ, Jezzard P, Duyn J, Frank JA, McLaughlin AC. Perfusion imaging of the human brain at 1.5 Tesla using a single shot EPI spin tagging approach. *Magn Reson Med* 1996; 36:219-224.
15. Yang Y, Frank JA, Hou L, Ye F, McLaughlin A, Duyn JH. Multislice imaging of cerebral perfusion with pulsed arterial spin-tagging. *Magn Reson Med* 1998; 39:825-832.
16. Kim SG, Tsekos NV. Perfusion imaging by a flow-sensitive alternating inversion recovery (FAIR) technique: application to functional brain imaging. 1997; 37:425-435.
17. Mattay VS, Frank JA, Santha AKS, et al. Whole brain functional mapping with isotropic MR imaging. *Radiology* 1996; 201:399-404.
18. Yang Y, Glover GH, Frank JA, et al. A comparison of fast MR scan techniques for cerebral activation studies at 1.5 Tesla. *Magn Reson Med* 1998; 39:61-67.
19. Bandettini PA, Jesmanowicz A, Wong EC, Hyde JS. Processing strategies for time course data sets in functional MRI of the human brain. *Magn Reson Med* 1993; 30:161-173.
20. Mueller WM, Yetkin FZ, Hammeke TA, et al. Functional magnetic resonance imaging mapping of the motor cortex in patients with cerebral tumors. *Neurosurgery* 1996; 39:515-520.
21. Cox RW, Jesmanowicz A, Hyde JS. Real-time functional magnetic resonance imaging. *Magn Reson Med* 1995; 33:230-236.
22. Yang Y, Glover GH, van Gelderen P, et al. Fast 3D functional magnetic resonance imaging at 1.5 T with spiral acquisition. *Magn Reson Med* 1996; 36:620-626.
23. Atlas SW, Howard RS II, Maldjian J, et al. Functional magnetic resonance imaging of regional brain activity in patients with intracerebral gliomas: findings and implications for clinical management. *Neurosurgery* 1996; 38:329-338.
24. Duyn JH, Yang Y. Single shot spiral functional MRI with trapezoidal gradients. *J Magn Reson* 1997; 128:130-134.
25. Cosgrove GR, Buchbinder BR, Jiang H. Functional magnetic resonance imaging for intracranial navigation. *Neurosurg Clin North Am* 1996; 7:313-322.
26. Kerr AB, Pauly JM, Hu BS, et al. Real-time interactive MRI on a conventional scanner. *Magn Reson Med* 1997; 38:355-367.
27. Jackson JJ, Meyer CH, Nishimura DG, Macovski A. Selection of a convolution function for Fourier inversion using gridding. *IEEE Trans Med Imaging* 1991; 10:473-478.
28. Ostuni J, Levin R, Frank JA, DeCarli C. Correspondence of closest edge voxels: a robust registration algorithm. *JMRI* 1997; 7:410-415.
29. Ostergaard L, Weisskoff RM, Chesler DA, Gyldensted C, Rosen BR. High resolution measurement of cerebral blood flow using intravascular tracer bolus passages. I. Mathematical approach and statistical analysis. *Magn Reson Med* 1996; 36:715-725.
30. Ostergaard L, Sorensen AG, Kwong KK, Weisskoff RM, Gyldensted C, Rosen BR. High resolution measurement of cerebral blood flow using intravascular tracer bolus passages. II. Experimental comparison

- and preliminary results. *Magn Reson Med* 1996; 36:726-736.
31. Alsop DC, Detre JA. Reduced transit-time sensitivity in noninvasive magnetic resonance imaging of human cerebral blood flow. *J Cereb Blood Flow Metab* 1996; 16:1236-1249.
 32. Ostuni JL, Santha AKS, Mattay VS, Weinberger DR, Levin RL, Frank JA. Analysis of interpolation effects in the reslicing of functional MR images. *J Comput Assist Tomogr* 1997; 21:803-810.
 33. Gold S, Christian B, Arndt S, et al. Functional MRI statistical software packages: a comparative analysis. *Hum Brain Map* 1998; 6:73-84.
 34. Cox RW. AFNI: software for analysis and visualization of functional magnetic resonance neuroimages. *Comput Biomed Res* 1996; 29:162-173.
 35. Hacklander T, Reichenbach JR, Weule J, Modder U. An efficient and robust PC program to calculate MR based regional cerebral blood volume maps. *Comput Med Imaging Graph* 1997; 21:51-62.
 36. Hesser J, Manner R, Braus DF, Ende G, Henn FA. Real-time direct volume rendering in functional magnetic resonance imaging. *MAGMA* 1997; 5:87-91.
 37. Duyn JH, Frank JA, Moonen CTW. Incorporation of lactate measurement in multi-spin-echo proton spectroscopic imaging. *Magn Reson Med* 1995; 33:101-107.
 38. Buckner RL, Bandettini PA, O'Craven KM, et al. Detection of cortical activation during averaged single trials of a cognitive task using functional magnetic resonance imaging. *Proc Natl Acad Sci USA* 1996; 93:14878-14883.
 39. Pocock SJ. *Clinical trials: a practical approach*. Wiley, New York, NY: 1983; 146-159.
 40. Moriarty TM, Kikinis R, Jolez FA, Black PM, Alexander E III. Magnetic resonance imaging therapy. *Neurosurg Clin North Am* 1996; 7:323-331.
 41. Pearlman JD, Edelman RR. Ultrafast magnetic resonance imaging segmented turboFLASH, echo-planar and real time nuclear magnetic resonance. *Radiol Clin North Am* 1994; 32:593-612.
 42. Leung DA, Debating J., Wildermuth S, et al. Real-time biplanar needle tracking for interventional MR imaging procedures. *Radiology* 1995; 197:485-488.
 43. Kasner SE, Grotta JC. Emergency identification and treatment of acute ischemic stroke. *Ann Emerg Med* 1997; 30:642-653.
 44. Albers GW. Rationale for early intervention in acute stroke. *Am J Cardiol* 1997; 80:4D-10D.